Food and Bioprocess Technology (2023) 16:2147–2158
https://doi.org/10.1007/s11947-023-03058-5

RESEARCH

Comparative Study of Cinnamon and Paprika Oleoresins Encapsulated by Spray Chilling and Particles from Gas Saturated Solutions Techniques: Evaluation of Physical Characteristics and Oleoresins Release in Food Simulated Media

Fernanda Ramalho Procopio[1] · Stefan Klettenhammer[2] · Giovanna Ferrentino[2] · Matteo Scampicchio[2] · Paulo José do Amaral Sobral[3,4] · Miriam Dupas Hubinger[1]

Received: 12 September 2022 / Accepted: 3 March 2023 / Published online: 13 March 2023

Abstract
In this study, cinnamon and paprika oleoresins were encapsulated by two technologies, respectively, spray chilling and particles from gas saturated solutions. Both technologies used palm oil as wall materials. The physical characteristics of the microparticles were compared as well as the oleoresins release behavior in high- and low-fat simulated food media. The spray chilling microparticles had an average diameter of 143.7 ± 1.5 µm, spherical shape, smooth surface, and passable flow property. In contrast, microparticles obtained by particles from gas saturated solutions (PGSS) showed an average diameter of 105.7 ± 0.6 µm, irregular shape, porous surface, poor flow property but higher encapsulation efficiency. In evaluating the compounds released in a simulated food medium, the spray chilling particles delivered 30.7%, while PGSS reached 23.1% after 1 h. Both microparticles well fitted the Kosmeyer-Peppas ($R^2 = 0.98$ and 0.96 for spray chilling and PGSS) and Peppas-Sahlin models ($R^2 = 0.98$ and 0.97 for spray chilling and PGSS). However, spray chilling microparticles showed a diffusion mechanism, while for PGSS ones erosion was the main mechanism. Despite the different physical characteristics, both microparticles proved to be possible facilitators in delivering oleoresins in food products.

Keywords Spray chilling · Particles from gas saturated solutions · Oleoresins · Lipid carriers · Physical properties · Controlled release

Introduction

The color and flavor of food products designate an essential task of attractiveness and quality sign to the consumer. With the intensified search for a healthier life and the consumption of foods with natural appeal, the food industry faces the challenge of finding new ingredients that meet this demand (Solymosi et al., 2015). Among these ingredients, oleoresins have stood out. Oleoresins are natural extracts obtained from plants and spices, such as cinnamon and paprika, comprising several bioactive compounds. Cinnamon oleoresin is characterized by volatile compounds, such as cinnamaldehyde, which are responsible for the aroma of the raw material. On the other side, paprika oleoresin is mainly composed of carotenoids, which are natural pigments widely used as colorants in the food industry (Procopio et al., 2022). As they have fractions of volatile and non-volatile compounds, oleoresins have a higher biological activity (i.e., antioxidant, antimicrobial, anti-inflammatory) compare to essential oils. Nevertheless, the loss of these compounds must be avoided during processing and storage. However, the viscosity, low water solubility, and incompatibility with some lipids impair the direct incorporation of these extracts in foods (Oriani et al., 2016; Sowbhagya, 2019). Microencapsulation has

✉ Giovanna Ferrentino
giovanna.ferrentino@unibz.it

1 Laboratory of Process Engineering, Department of Food Engineering, School of Food Engineering, University of Campinas, Campinas, SP 13083-862, Brazil

2 Faculty of Science and Technology, Free University of Bozen-Bolzano, Piazza Università 5, 39100 Bolzano, Italy

3 Department of Food Engineering, Faculty of Animal Science and Food Engineering, University of São Paulo, Av Duque de Caxias Norte, Pirassununga, SP 225, 13635-900, Brazil

4 Food Research Center (FoRC), University of São Paulo, Rua Do Lago, 250, Semi-Industrial Building, Block C, São Paulo, SP 05508-080, Brazil

been used to ease the addition of oleoresins in food products besides to contribute to increase their shelf life (Aberkane et al., 2014; Pourashouri et al., 2014; Ndayishimiye et al., 2019). Spray drying remains the most used encapsulation technique. Several studies can be found in the literature where investigations on the effect of the wall material on the physical properties and release behavior of the microcapsules are carried out (Bucurescu et al., 2018; Estevinho et al., 2021; Fu et al., 2020; Oliveira et al., 2018; Ribeiro et al., 2019). Among the wall materials, gum, maltodextrin, protein isolates, and modified starches are the most frequently used.

However, in food technology, the use of lipid carriers for oleoresins encapsulation remains still unexplored. Lipid carriers have some advantages compared to some wall materials such as the lower toxicity, the ability to increase the oral bioavailability of the encapsulated compounds and to improve or control their release (Ganesan & Narayanasamy, 2017; Harde et al., 2011). As an example, Fadini et al. (2018) combined spray drying and spray chilling techniques to use lipid carriers as an outer layer in particles to deliver fish oil, masking the taste and decreasing the solubility of the particles in water. Spray chilling is one of the conventional microencapsulation techniques applied to obtain microparticles with lipid carriers as wall material. The process is typically run in spray dryer equipment. The melted lipid carriers holding the active ingredient are atomized in a cold chamber (temperature below the lipid melting point), and the particles are formed by the lipid crystallization (Alvim et al., 2016; Bampi et al., 2016). Usually, spray chilling particles are classified as microspheres, where the active ingredient is dispersed in the matrix, presenting a round and smooth surface (Figueiredo et al., 2022). Ascorbic acid, curcumin, capsaicin, cinnamon, and ginger oleoresins are examples of some bioactive ingredients encapsulated by spray chilling technique (Sorita et al., 2021; Gunel et al., 2021; de Matos-Junior et al., 2017; Carvalho et al., 2019; Oriani et al., 2018; Procopio et al., 2018). In most of the published studies on spray chilling microparticles, the effect of the processing variables and the application of different wall materials have been investigated as key features impacting on the physical characteristics of the microparticles (Paulo & Santos, 2020). However, aspects related to the mechanisms of compounds release from the microparticles to food simulating media have not been in deep addressed. On the contrary, such aspects are widely discussed in powders produced by spray drying. As an example, in the work of Ribeiro et al. (2019), microparticles incorporating polyphenols were produced by spray drying. The kinetics of polyphenol release was studied by applying the zero order, the Korsmeyer-Peppas, and the Weibull models.

Besides conventional microencapsulation technique, recently novel processes based on the use of supercritical carbon dioxide are emerging. Among them, the particles from gas saturated solutions (PGSS) technique represents one of the most attractive. It uses carbon dioxide (CO_2) in the supercritical state to solubilize the mixture formed by the carrier and the active ingredient. The process involves the saturation of this mixture with CO_2, followed by the rapid expansion at atmospheric pressure. When the expansion occurs through an atomizing nozzle, it causes a cooling effect that allows the lipid material to crystallize and obtain solid microparticles (Klettenhammer et al., 2020). As for the spray chilling, PGSS involves the use of lipid carriers. It has the advantage to be solvent-free and easy to scale industrially. Several studies demonstrated the potential of the technology to encapsulate bioactive compounds (Haq & Chun, 2018; Klettenhammer et al., 2022; Ndayishimiye et al., 2019). As an example, Ndayishimiye et al. (2019) encapsulated oils recovered from brewer's spent grain (Ferrentino et al., 2019) by PGSS choosing polyethylene glycol as wall material. Klettenhammer et al. (2022) used purified sunflower wax to encapsulate linseed oil and enriched the microparticles with carrot pomace extract obtaining a final product with enhanced oxidative stability. In most of the published studies, the superior features of the obtained microparticles are claimed, although no direct comparison with those produced by a conventional encapsulation technique has been ever performed. Moreover, aspects related to the compounds release from the microparticles to food simulating media have never been addressed.

The present work is the first attempt to cover the gap of knowledge related to microparticles produced using lipid carriers as wall material by conventional and innovative technologies. To this extent, cinnamon and paprika oleoresins were encapsulated by spray chilling using lipid carriers as wall material. The obtained microparticles were then compared to those produced by PGSS technique. After their production, microparticles were characterized by size, morphology, encapsulation efficiency, and flowability. Their release behavior was also studied by fitting the kinetics with appropriate mathematical models.

Material and Methods

Production of Solid Lipid Microparticles

Spray Chilling

Solid lipid microparticles (SLMs) were obtained using a Büchi-B290 spray dryer set in spray chiller mode (Büchi, Flawil, Switzerland) according to Procopio et al. (2018). The layout of the process is shown in Fig. 1. Fully hydrogenated palm oil (Triângulo Alimentos, Itápolis, Brazil) and palm fat (Cargill,

Mairinque/São Paulo, Brazil) were mixed (80:20, w/w) (100 g) and heated up to 70 °C by a temperature-controlled water bath (Tecnal, TE-184, Piracicaba, Brazil) to assure complete melting. Then, the cinnamon and paprika oleoresins (2:1, w/w) (3 g) (Synthite, Valinhos/Sao Paulo, Brazil) were weighted, and the melted lipids were added until reaching the final amount of 100 g. Feeding to the heated double fluid atomizer (nozzle diameter of 0.7 mm) was done by a peristaltic pump at a mass flow rate of 0.7 kg/h. During pumping, the feeding tube was kept warm to avoid any blocking. Using the dehumidifier accessory B-296 (Büchi, Flawil, Switzerland), ambient air (24.2 °C, 41.2% relative humidity) was cooled and used as inlet air conditioning. Atomizing air and cooling airflow rates were 831 L/h and 35.000 L/h, respectively. In such conditions, the inlet and outlet temperatures of cooling air were 6 ± 1 °C and 10 ± 2 °C, respectively. At the end of the process, samples were collected, stored in closed containers, and kept at room temperature. Each experiment was performed in duplicate.

Particles from Gas Saturated Solutions

The same formulation prepared for the spray chilling was used to produce SLMs by PGSS, following the methodology described by Klettenhammer et al. (2022) with small changes. In addition, a control formulation formed only by the carrier materials was produced to obtain a comparison parameter. The layout of the process is shown in Fig. 2. The mixture (10 g) was placed inside a heated (55 °C) stainless-steel reactor. Preliminary experiments were carried out to identify the best processing pressure. PGSS was performed at 10, 20, and 30 MPa. A pressure of 10 MPa showed unsatisfactory solubilization of oleoresins in the carrier materials forming agglomerates. Further experiments were performed at 20 and 30 MPa to ensure better solubilization and atomization conditions. The obtained samples reported better encapsulation efficiency, no agglomerates, and no significant differences between the two pressures. Thus, an operative pressure of 20 MPa was chosen for the experiments of the present study. At this pressure, CO_2 was pumped inside the preheated reactor reaching the supercritical state and becoming able to melt the mixture. Melting and solubilization of the melted mixture continued until saturation conditions were achieved in supercritical CO_2. After 1 h, the outlet valve of the reactor was opened, and the supercritical mixture was sprayed through a nozzle of 600 µm into a cyclone chamber at atmospheric pressure. The heating of the nozzle was turned on for 10 min before opening the valve of the reactor to reach 55 °C. The values of time and temperature were chosen based on preliminary experiments. The samples were prepared in duplicate and analyzed during the week.

Characterization of Solid Lipid Microparticles

Total Carotenoid Content

Microparticles (100 mg) were added to 20 mL of hexane for carotenoids extraction. The samples were then diluted 10 times, and the absorbances were read with a spectrophotometer (Cary 100 Series UV–Vis Spectrophotometer, Agilent Technologies, Italy) at 472 and 508 nm (Hornero & Míngues, 2001). The isochromatic red and yellow fractions and the total carotenoid content were calculated using Eqs. (1), (2), and (3), respectively.

$$C^R = \frac{A_{508}x2144.0 - A_{472}x403.3}{270.9} \quad (1)$$

$$C^Y = \frac{A_{472}x1724.3 - A_{508}x403.3}{270.9} \quad (2)$$

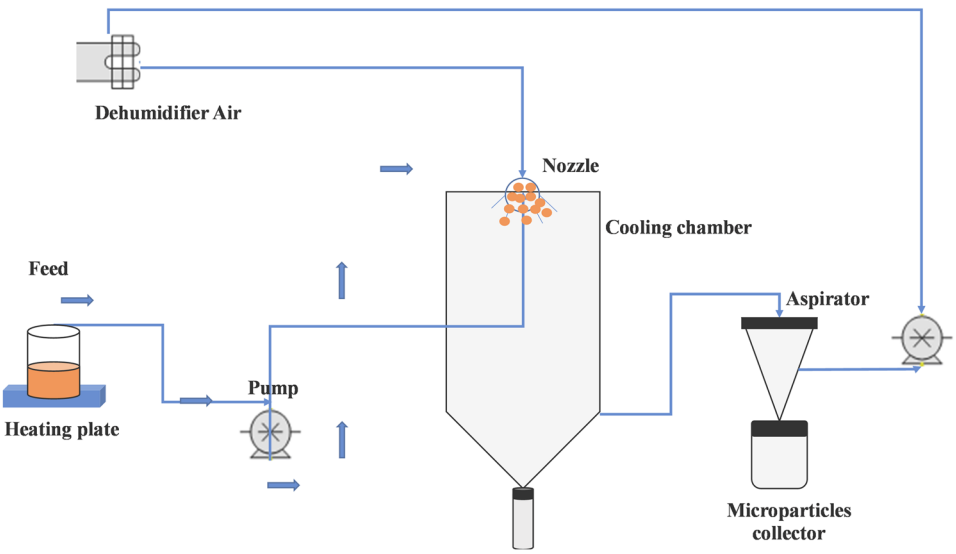

Fig. 1 Layout of spray chilling process

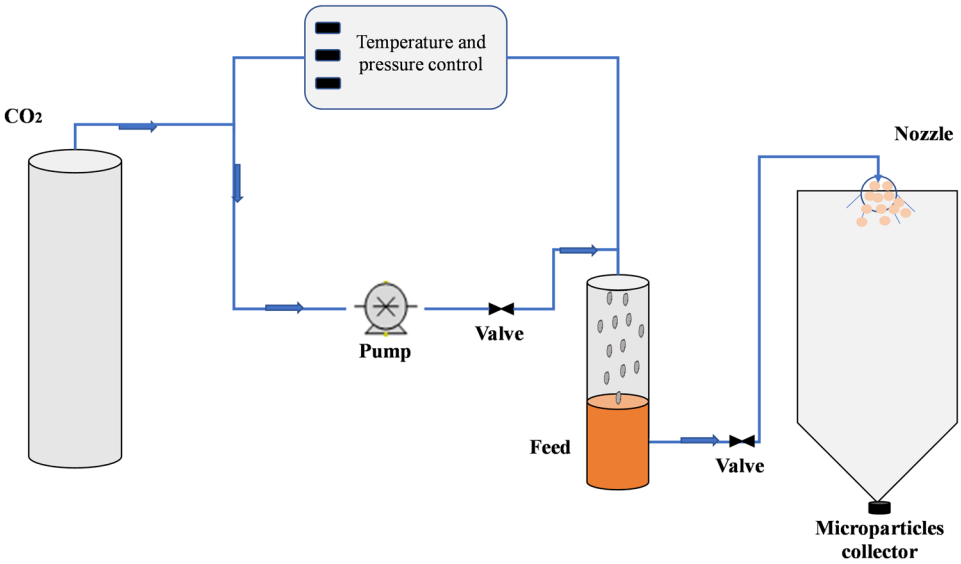

Fig. 2 Layout of particles from gas saturated solution process

$$C^T = C^R + C^Y \tag{3}$$

where C^R represented the content of the isochromatic red fraction, C^Y represented the yellow isochromatic fraction, C^T represented the total carotenoid content, and A_{472} and A_{508} were the absorbance values at 472 nm and 508 nm, respectively.

Bulk Density, Tapped Density, Cohesiveness, and Flowability

For the determination of bulk density, a 10 mL graduated cylinder was filled with the powders, according to Caliskan and Dirim (2016) with modifications. Bulk density (ρ_{bulk}) was calculated by the ratio of mass to the measured volume read directly from the cylinder. In order to determine the tapped density (ρ_{tapped}) of microparticles, the cylinder was tapped until the constant volume of the sample was read. Flowability and cohesiveness values of the powders were evaluated in terms of the Carr index (CI) and Hausner ratio (HR), respectively. Both CI and HR were calculated from the bulk (ρ_{bulk}) and tapped (ρ_{tapped}) densities of the microparticles using the followings Eqs. (4) and (5), respectively:

$$CI = \frac{(\rho_{tapped} - \rho_{bulk})}{\rho_{tapped}} x100 \tag{4}$$

$$HR = \frac{\rho_{tapped}}{\rho_{bulk}} \tag{5}$$

Color

Color measurements were performed using a colorimeter (Minolta Chroma Meter II Reflectance CR-300, Milano, Italy) and expressed with the CIELab scale (L^*, a^*, b^*). The lightness value (L^*) indicated the darkness/lightness of the sample, a^* was a measurement of the greenness/redness of the sample, and b^* was the extent of blueness/yellowness. The color difference ΔE^* was calculated following Eq. 6, using L_0^*, a_0^*, and b_0^* of the control (the sprayed wall material without the oleoresins). The samples were uniformly distributed in a Petri plate. The measurements were performed in duplicate, and the results were expressed as mean values and standard deviations.

$$\Delta E^* = \sqrt{\left[\left(L^* - L_0^*\right)^2 + \left(a^* - a_0^*\right)^2 + \left(b - b_0^*\right)^2\right]} \tag{6}$$

Particle Size Distribution

The size distribution and the polydispersity index (span) of the microparticles were determined by a light scattering technique using a laser diffraction in a Mastersizer Hydro 3000 with water as a dispersant medium (Malvern Instruments Ltd., Malvern, Worcestershire, UK). The analysis was performed in triplicate at room temperature. The mean surface diameter $D_{[4,3]}$, the mean volume diameter $D_{[3,2]}$, and the size distribution characterized by $D_{[0.1]}$, $D_{[0.5]}$, and $D_{[0.9]}$, representing the diameter of the accumulated distribution of 10%, 50%, and 90% of total microparticles, respectively, were reported as mean values and standard deviations.

Morphology

The morphology of the microparticles was analyzed by scanning electron microscopy (SEM) using a Phenom™ ProX SEM (Eindhoven, The Netherlands) electron microscope (Paulo & Santos, 2019). These analyses were performed with an accelerating voltage of 15 kV at room temperature and under vacuum. Micrographs were obtained with magnifications of 940× and 980×. The images of the samples were captured by the ProSuite (Eindhoven, The Netherlands) application platform and saved in tiff format resulting in 2048 × 2176 pixels. Particle Metric software was used to measure the particle size, with the following detection settings: 0.10 (minimum contrast), 0.10 (merge shared borders), 0.3 (conductance), and 1.5% (minimum detection size).

Encapsulation Efficiency

The encapsulation efficiency was defined as the total amount of encapsulated carotenoids (m_e) divided by the total amount of carotenoids in the lipid mixture (before the encapsulation process, m_t) as reported in Eq. 7:

$$EE\% = \frac{m_e}{m_t} \times 100 \tag{7}$$

Oleoresins Release in Food Simulant Media

To investigate the oleoresins release in food simulated media, 10 mg of the powders were weighted and added to 40 mL glass vials containing 5 mL of 30% (Benbettaïeb et al., 2016) or 95% (Chen et al., 2012) ethanol solutions, prepared in water, representing a low- and high-fat food simulant, respectively. A total of 9 glass vials (in duplicate), each of them corresponding to a release time, were prepared and kept under orbital stirring (100 rpm) according to Hoseyni et al. (2021). For each realizing time, the entire content of the vial (5 mL) was then filtered using 5 mL syringes with 0.25 mm filters. The absorbance of the solution was read at 450 nm. Experiments were performed in duplicate, and the results were expressed as mean values and standard deviation.

Modeling Oleoresins Release Data

To determine the kinetics of oleoresins release in food simulant media, data were analyzed using zero order (Eq. 8), first order (Eq. 9), Higuchi (Eq. 10), Korsmeyer-Peppas (Eq. 11), Peppas-Sahlin (Eq. 12), and Kopcha (Eq. 13) models:

$$Q_t = Q_0 + Kt \tag{8}$$

$$lnQ_t = lnQ_0 - Kt \tag{9}$$

$$Q_t = K\sqrt[2]{t} \tag{10}$$

$$Q_t = Kt^n \tag{11}$$

$$Q_t = K_1 t^m + K_2 t^{2m} \tag{12}$$

$$Q_t = K_1 t^{0.5} + K_2 t \tag{13}$$

where Q_t is the amount (%) of compounds released at time t and K is the kinetics constant, in Eqs. 7, 8, 9, and 10. In Eq. 10, n is the release coefficient. For spherical particles, when $n = 0.43$, the release follows a Fickian diffusion, for $0.43 < n < 0.85$ a non-Fickian diffusion, while if $n = 0.89$, the case II transport is predominant (Korsmeyer et al., 1983). In Eqs. 11 and 12, K_1 is the diffusion rate constant (Fickian), K_2 is the erosion rate constant, and m is the purely Fickian diffusion exponent for a system of any configuration. When $K_1/K_2 > 1$, the diffusion mechanism is predominant; for $K_1/K_2 < 1$, the erosion mechanism is predominant; and if $K_1/K_2 = 1$, both mechanisms are present.

Statistical Analysis

All the results were expressed as mean values followed by the standard deviation of two or more independent experiments. Data were statistically analyzed by Tukey's test (p-value ˂ 0.05) using the trial edition of the Minitab software (Minitab 180, Minitab Inc., State College, PA, USA).

Results and Discussion

Color and Total Carotenoid Content

Carotenoids are recognized as one of the most important natural food colorants used in the food industry (Martins et al., 2016). The total carotenoid content was the same for both processes with no significant statistical differences ($p < 0.05$). The color of carotenoids rich powders is an important indicator of quality and applicability. Regarding the color parameters (Table 1), the spray chilling microparticles reported a stronger orange color with 60.6 ± 1.1 for the yellowness indicator (b^*), 38.8 ± 1.4 for the redness (a^*), and 66.5 ± 1.0 of lightness (L^*), with the highest difference from the sprayed wall material without the oleoresins

Table 1 Color parameters and microparticles total carotenoids content

Sample	L^*	a^*	b^*	ΔE_1	ΔE_2	Total carotenoids content (mg of carotenoid/g of sample)
Spray chilling	66.5 ± 1.0^c	38.8 ± 1.4^a	60.6 ± 1.1^a	71.5 ± 2.2^a	76.1 ± 0.1	0.6 ± 0.1^a
PGSS	82.4 ± 1.0^b	19.4 ± 1.2^b	33.6 ± 1.4^b	36.1 ± 2.1^b	39.4 ± 2.1	0.6 ± 0.1^a
Control[1]	95.1 ± 1.0^a	1.90 ± 0.4^c	6.5 ± 0.8^c	-	5.3 ± 0.1	-

Different lowercase letters in the same column represent a statistically significant difference ($p \leq 0.05$)

[1]Sprayed wall material without the oleoresins. $\Delta E_{1:}$ color difference between samples and the sprayed wall material without the oleoresins; $\Delta E_{1:}$ color difference between samples and a standard white plate

defined as the control in Fig. 3 ($\Delta E = 71.5 \pm 2.2$). The PGSS was light orange, with a b^* value of 33.6 ± 1.4, 19.4 ± 1.2 for a^*, and 82.4 ± 1.0 of lightness (L^*). Results were in agreement with the visual aspect observed in the samples (Fig. 3). Particle size and porosity can influence powder color and lightness due to the light scattering phenomenon (Nabil et al., 2020). Also, the presence of more carotenoids in the surface can increase the color saturation. Haas et al. (2019) encapsulated carotenoids by spray drying and freeze drying technologies and observed that L^* values increased for smaller particles, while a^* and b^* values increased for larger particles. The same behavior was observed for the PGSS particles in this study, which showed a porous structure, smaller diameter, higher brightness, and lighter color.

Yield, Encapsulation Efficiency, and Flowability

Table 2 shows the physical parameters of the microparticles produced by the two different encapsulation techniques. No statistical differences were found for the yield. Particles from spray chilling and PGSS showed $76.4 \pm 8.1\%$ and $93.0 \pm 4.4\%$ of encapsulation efficiency, respectively. The values indicated that for the microparticles produced by PGSS, the oleoresins were better encapsulated inside the wall material. With the same total carotenoid content but with lower encapsulation efficiency, the spray chilling microparticles confirmed the higher amounts of the active ingredient on the particles surface (Okuro et al., 2013). This result also explained the light color parameters for the PGSS microparticles due to the oleoresins, which were more embedded within the wall material.

The flowability of microparticles is determined by the correlation between tapped and bulk density, expressed as the Carr index (CI) and the Hausner ratio (HR). According to the US Pharmacopeia, the flowability of materials is classified as excellent with CI values below 10, good with values between 11 and 15, fair between 16 and 20, passable between 21 and 25, poor between 26 and 31, very poor between 32 and 37, and very, very poor higher than 38. The microparticles produced by spray chilling technique showed higher values of bulk (0.30 ± 0.01 g/cm^3) and tapped density (0.40 ± 0.01 g/cm^3), and a Carr index of 24.7 ± 0.8 reporting a classification of powders with a passable flow property. The microparticles from gas saturated solutions had a finer granulometry with a bulk density of 0.07 ± 0.02 g/cm^3, tapped density of 0.09 ± 0.02 g/cm^3, and CI of 28.1 ± 0.2, classified as samples with poor flow properties. According to Wolska (2021), fine lipid powders generally present inferior flowability. The particle size, morphology, lipid material, and processing conditions can directly influence flow properties. In a study developed by Gunel et al. (2021), spray chilling was used for the microencapsulation of capsaicin emulsified with palm oil, sunflower seed oil, whey protein isolates, and soy lecithin. The powder presented a very poor flowability, with a Carr index of 48.9 ± 0.2. Klettenhammer et al. (2022) founded Carr index values between 12.5 and 25.1 for the linseed oil encapsulated by PGSS with different pressure conditions (10–30 MPa) and sunflower wax (85 °C) as wall material. They observed that particles produced using 10 MPa presented the best flow property with a Carr index of $12.5 \pm 0.25\%$. The low melting point of the

Fig. 3 Visual aspect of the microparticles

Table 2 Physical parameters of the microparticles

Property	Spray chilling	PGSS
Yield (%)	74.9 ± 0.7^a	70.0 ± 5.7^a
Encapsulation efficiency (%)	76.4 ± 8.1^b	93.0 ± 4.4^a
Bulk density (g/cm^3)	0.30 ± 0.01^a	0.07 ± 0.02^b
Tapped density (g/cm^3)	0.40 ± 0.01^a	0.09 ± 0.02^b
Carr index	24.7 ± 0.8^b	28.1 ± 0.2^a

Different lowercase letters in each line represent a statistically significant difference ($p \leq 0.05$)

lipid materials used in the present study (~ 50 °C) may have influenced the formation of agglomerates, which also contributed to a reduction in the flow properties.

Morphology and Particle Size Distribution

The morphology of microparticles obtained by spray chilling and PGSS is shown in Fig. 4. The particles produced by spray chilling presented a spherical shape, smooth surface, and no porous and agglomerated clusters, with small particles adhered to bigger ones. The particles from PGSS presented irregular and variated shape, porous surface, and a higher amount of particle agglomeration. Size and morphology characteristics are influenced by the microencapsulation process conditions and by the core/wall materials. Generally, spray chilling microparticles present spherical and smooth surface (Consoli et al., 2016; Oriani et al., 2018; Procopio et al., 2018), while supercritical encapsulation techniques report difficulty in controlling morphology due to the rapid expansion rate during the process (Haas et al., 2019; Janiszewska-Turak, 2017; Klettenhammer et al., 2022; Ndayishimiye & Chun, 2018).

The particle size distribution of the microparticles is presented in Table 3. Spray chilling sample presented bigger particles, with $D_{[4,3]}$, D_{50}, and span values of 333.3 ± 2.1 µm, 143.7 ± 1.5 µm, and 6.0 ± 1.0, respectively, while PGSS samples reported values of 291.3 ± 0.6 µm, 105.7 ± 0.6 µm, and 7.5 ± 0.5, respectively.

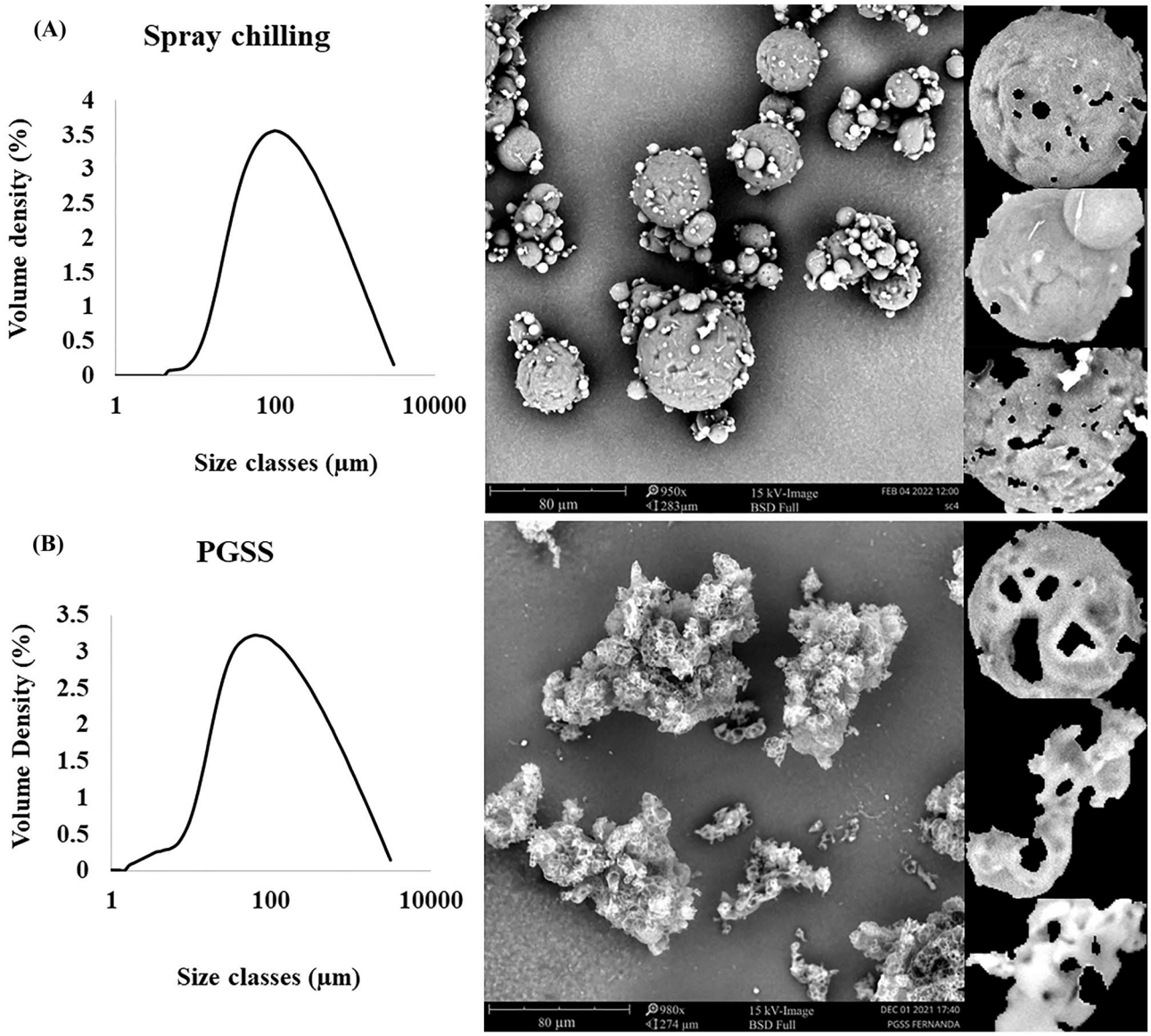

Fig. 4 Size distribution and scanning electron micrographs (950 × and 980 ×) of spray chilling **A** and PGSS **B** microparticles

Table 3 Particle size distribution and particle metric image analysis for spray chilling and PGSS microparticles

Property	Spray chilling	PGSS
$D_{[4,3]}$ (μm)	333.3 ± 2.1^a	291.3 ± 0.6^b
$D_{[3,2]}$ (μm)	73.5 ± 0.5^a	43.0 ± 0.9^b
D_{10} (μm)	29.6 ± 0.2^a	19.4 ± 0.5^b
D_{50} (μm)	143.7 ± 1.5^a	105.7 ± 0.6^b
D_{90} (μm)	896.3 ± 5.5^a	809.3 ± 3.2^b
Span	6.0 ± 1.0^b	7.5 ± 0.5^a
Circle equivalent diameter (μm)	35.1 ± 1.1^a	18.8 ± 1.5^b
Circumference (μm)	158 ± 2.5^a	104 ± 1.9^b
Circularity	0.55 ± 0.03^a	0.39 ± 0.01^b
Convexity	0.81 ± 0.02^a	0.77 ± 0.03^b
Elongation	0.17 ± 0.01^b	0.38 ± 0.02^a

Different uppercase letters in the same raw represent a statistically significant difference ($p \leq 0.05$)

Particle size characterization was also performed by image microscope analysis (Table 3). According to Wejrzanowski et al. (2006), image microscope analysis is a direct method for the determination of powder material size and is focused on the geometry of individual particles. On the other hand, laser diffraction is an indirect measurement method based on physical effects. The type of dispersant and dispersibility of the particles in the media can affect the reading and must be taken into account. As shown in Table 3, the mean diameter of the spray chilling microparticles was 143.7 ± 1.5 μm. Using the particle metric program to analyze the SEM images, a similar value was found for the average circumference, 158 ± 2.5 μm. For microparticles produced by PGSS, the mean diameter value determined by laser diffraction was 105.7 ± 0.6 μm, while the average circumference was 104 ± 1.9 μm by image analysis (Table 3). In addition, particles produced by spray chilling technique presented higher circularity and lower elongation (0.55 ± 0.03 and 0.16 ± 0.01, respectively) compared to PGSS microparticles (0.39 ± 0.01 and 0.38 ± 0.02, respectively). The results are confirmed by the morphologies observed in Fig. 4A and B.

Oleoresins Release from Microparticles in Food Simulant Media

Figure 5 shows oleoresins release in a high-fat (95% ethanol) and low-fat (30% ethanol) food simulant. Concerning the results in high-fat medium, the spray chilling microparticles reached a 30.7% release over a period of 1 h, while the PGSS presented a release equal to 23.1%. The higher release of compounds from spray chilling microparticles could be related to the presence of more oleoresin on the surface of the particle confirmed by the encapsulation efficiency results. Also, the greater solubility of the compounds in the medium contributes to a faster release, as observed by Benković et al. (2021). The authors evaluated the water release of *Lamiaceae* extracts through alginate microbeads. The curves showed an accelerated phase in the first 20 min, followed by a second phase where the concentration difference was less significant.

The percentage of carotenoids released from the spray chilling microparticles was higher than PGSS ones. The increase in the dispersibility of hydrophobic compounds in aqueous media depends on the type of microencapsulation processes (Santos et al., 2021). In the study of Oliveira et al. (2017), Pequi oil (naturally insoluble in water) was encapsulated by spray drying using different combinations of whey protein isolate (WPI), maltodextrin (MD), and chicory inulin (IN). These authors observed that the formulation containing inulin/WPI increased the solubility of the Pequi oil, allowing its addition in an aqueous medium.

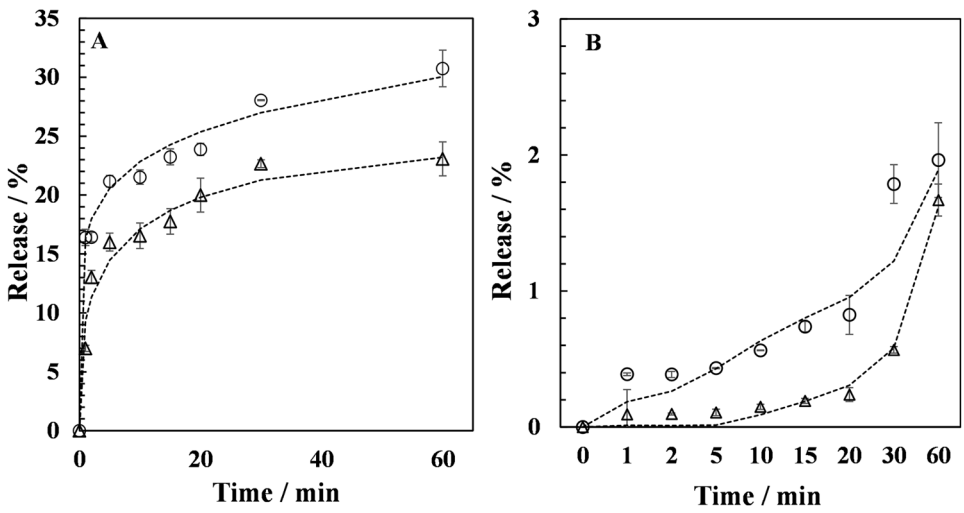

Fig. 5 Release of oleoresins in high-fat simulant medium (95% ethanol) **A** and low-fat simulant medium (30% ethanol) **B**. Symbols are ○, spray chilling microparticles; Δ, PGSS microparticles. Dotted lines are the Kosmeyer-Peppas model

Table 4 Modeling parameters for the release in high-fat (95% ethanol) food simulant

	K_1		K_2		n or m		R^2	
Model	Spray chilling	PGSS	Spray chilling	PGSS	Spray chilling	PGSS	Spray chilling	PGSS
Zero order	0.74	0.57	Nd	nd	nd	nd	0.70	0.72
First order	−0.01	−0.03	Nd	nd	nd	nd	0.86	0.68
Higuchi	5.24	3.98	Nd	nd	nd	nd	0.85	0.88
Kupcha	9.92	7.25	−0.81	−0.57	nd	nd	0.91	0.95
Kosmeyer-Peppas	16.21	10.13	nd	nd	0.15	0.21	0.98	0.96
Peppas-Sahlin	11.77	10.47	4.50	−1.16	0.11	0.33	0.98	0.97

K_1 and K_2 release rate constants, n and m release coefficients, R^2 correlation coefficient, *nd* not determined

The results of low-fat simulant media (Fig. 5B) indicated a delay in the release from the PGSS microparticles. The percentage of oleoresin released was practically the same during the first 15 min, going from 0.27 to 0.57% during 30 min and reaching a maximum of 1.67% after 1 h. The low solubility of carotenoids in water could explain the fact that the release was significantly greater in the high-fat than in the low-fat medium. Similar results were reported by Kevij et al. (2020) studying the release of curcumin from whey protein isolate-based films in high-fat (95% ethanol) and semi-fat (50% ethanol) food simulants. After 210 h of shaking, the percentage of curcumin reached 53.7% in 95% ethanol and 24.3% in 50% ethanol for the formulations containing 0.2 mg of the bioactive/mL.

By modeling the oleoresins release, the zero order (Eq. 7), first order (Eq. 8), Higuchi (Eq. 9), Kupcha (Eq. 10), Kosmeyer-Peppas (Eq. 11), and Peppas-Sahlin (Eq. 12) models were fitted to the data by non-linear regression. The calculated parameters are shown in Tables 4 and 5. Coefficient of determination (R^2) values greater than 0.85 indicate that the model well fitted the experimental data (Hoseyni et al., 2021). The highest R^2 for the spray chilling and PGSS microparticles was obtained with the Kosmeyer-Peppas and Peppas-Sahlin for both food simulants. Kosmeyer-Peppas release parameters in the high-fat media demonstrated R^2 of 0.98 and 0.96 for spray chilling and PGSS microparticles, respectively. The correlation with the Peppas-Sahlin model was 0.98 for the spray chilling and 0.97 for PGSS.

Although the same model fitted with good agreement with the oleoresins release from the PGSS and spray chilling samples, different mechanisms were detected. In the Peppas-Sahlin model, the K_1 and K_2 are emission and degradation constants, respectively, and m is the purely Fickian diffusion exponent for a system of any configuration (films, cylinders, and spheres) (Peppas & Sahlin, 1989). The release results of spray chilling microparticles in 95% ethanol (Table 4) showed K_1 larger than K_2, indicating that the diffusion mechanism is predominant. For the PGSS sample, the release took place through the erosion mechanism, with $K_2 > K_1$. The morphological difference between the microparticles can explain this behavior. While the spray chilling microparticles presented a spherical and smooth surface, the PGSS showed pores and irregular shapes. According to Bruschi (2015), the active release strongly depends on the structure through which the diffusion takes place. This explains why the same compound sometimes presents different behaviors depending on the matrix where it is incorporated.

The n exponent in the Kosmeyer-Peppas model indicates the predominant release mechanism (Korsmeyer et al., 1983). Spray chilling microparticles in 30% ethanol (Table 5) presented an n value equal to 0.61 indicating a

Table 5 Modeling parameters for the release in low-fat (30% ethanol) food simulant

	K_1		K_2		n or m		R^2	
Model	Spray chilling	PGSS	Spray chilling	PGSS	Spray chilling	PGSS	Spray chilling	PGSS
Zero order	0.04	0.02	nd	nd	nd	nd	0.89	0.93
First order	−0.03	−0.02	nd	nd	nd	nd	0.89	0.88
Higuchi	0.23	0.13	nd	nd	nd	nd	0.89	0.80
Kupcha	0.23	0.13	2.98	2.00	nd	nd	0.89	0.80
Kosmeyer-Peppas	0.16	0.01	nd	nd	0.61	1.65	0.91	0.97
Peppas-Sahlin	0.12	−0.02	0.05	0.01	0.39	0.66	0.91	0.97

K_1 and K_2 release rate constants, n and m release coefficients, R^2 correlation coefficient, *nd* not determined

non-Fickian release. For the PGSS in 30% of ethanol, the *n* value was 1.96, which is related to a Super Case II transport. In this case, tension and breaking of the polymer occurs during the sorption process (Bruschi, 2015). Ritger and Peppas (1987) discussed that these limits should not be applied for polydisperse samples with a wide size distribution. The authors pointed out that a varied size distribution causes substantial acceleration of the transport at early times and a marked retardation of the transport for longer times. Similar behavior was observed in the study of Carvalho et al. (2019) where ascorbic acid was encapsulated by spray chilling technique using different ratios between fully hydrogenated palm oil/palm oil. The release in an aqueous medium was measured. The particles presented a spherical shape, continuous surface, and multimodal particle size distribution. The ascorbic acid release results showed *n* values less than 0.43 for the Kosmeyer-Peppas model and fitted better for the Higuchi model, indicating that the release followed a diffusion mechanism.

Conclusions

Encapsulation of oleoresins by spray chilling produced spherical particles with a smooth surface, strong orange color, and an average diameter of 143.7 μm. The particles produced by PGSS were irregular with a porous surface, light orange, and an average diameter of 105.7 μm. The spray chilling sample showed better flow properties than PGSS. However, a higher encapsulation efficiency was reported for the PGSS microparticles. The study of the oleoresins release was carried out by simulating a high-fat (95% ethanol) and a low-fat (30% ethanol) food medium. The highest release of compounds was through the spray chilling particles in 95% ethanol, reaching 30.74% after 1 h. The oleoresins release in the low-fat medium was delayed by 15 min for both spray chilling and PGSS microparticles. This result indicated that the microparticles could better control the delivery of these compounds to the food simulants. The Kosmeyer-Peppas and Peppas-Sahlin models best fitted the data for all samples. However, the microparticles showed different release mechanisms due to morphological differences. Despite the different physical characteristics, both structures proved to be possible facilitators in delivering the active compounds of the oleoresins in food products.

Acknowledgements The authors gratefully acknowledge "Conselho Nacional de Desenvolvimento Científico e Tecnológico (CNPq)" for the PhD assistantships (Fernanda Ramalho Procopio #141111/2018-6) and the productivity grants (Miriam Dupas Hubinger #306461/2017-0; Paulo J. A. Sobral #30.0799/2013-6). Miriam Dupas Hubinger thanks FAPESP for the thematic project FAPESP 2019/ 27354-3. The authors acknowledge the support from "Coordenação de Aperfeiçoamento de Pessoal de Nível Superior" (CAPES-Brazil; Finance code 001).

Author Contribution Fernanda Ramalho Procopio and Stefan Klettenhammer conducted the research and investigation process, specifically performing the experiments; Giovanna Ferrentino developed the design of the methodology, performed data collection, verified the overall replication and reproducibility of the experiments, and carried out the writing, review and editing of the manuscript; Matteo Scampicchio, Paulo José do Amaral Sobral, and Miriam Dupas Hubinger concepted and supervised the research activity.

Funding Open access funding provided by Libera Università di Bolzano within the CRUI-CARE Agreement.

Data Availability The authors confirm that the data supporting the findings of this study are available within the article.

Declarations

Conflict of Interest The authors declare no competing interests.

References

Aberkane, L., Roudaut, G., & Saurel, R. (2014). Encapsulation and oxidative stability of PUFA-rich oil microencapsulated by spray drying using pea protein and pectin. *Food and Biprocess Technology, 7*, 1505–1517. https://doi.org/10.1007/s11947-013-1202-9

Alvim, I. D., Stein, M. A., Koury, I. P., Dantas, F. B. H., & Cruz, C. L. C. V. (2016). Comparison between the spray drying and spray chilling microparticles contain ascorbic acid in a baked product application. *LWT, 65*, 689–694. https://doi.org/10.1016/j.lwt.2015.08.049

Bampi, G. B., Backes, G. T., Cansian, R. L., de Matos Jr., F. E., Ansolin, I. M. A., Poleto, B. C., Corezzolla, L. R., & Favaro-Trindade, C. S. (2016). Spray chilling microencapsulation of *Lactobacillus acidophilus* and *Bifidobacterium animalis* subsp. lactis and its use in the preparation of savory probiotic cereal bars. *Food and Bioprocess Technology, 9*, 1422–1428. https://doi.org/10.1007/s11947-016-1724-z

Benbettaïeb, N., Chambin, O., Karbowiak, T., & Debeaufort, F. (2016). Release behavior of quercetin from chitosan-fish gelatin edible films influenced by electron beam irradiation. *Food Control, 66*, 315–319. https://doi.org/10.1016/j.foodcont.2016.02.027

Benković, M., Sarić, I., Jurinjak Tušek, A., Jurina, T., Kljusurić, J. G., & Valinger, D. (2021). Analysis of the adsorption and release processes of bioactives from *Lamiaceae* plant extracts on alginate microbeads. *Food and Bioprocess Technolpgy, 14*, 1216–1230. https://doi.org/10.1007/s11947-021-02632-z

Bruschi, M. L. (2015). Mathematical models of drug release. In: Bruschi, M.L. Strategies to Modify the Drug Release from Pharmaceutical Systems, Woodhead Publishing, chapter 5, 63–86. https://doi.org/10.1016/B978-0-08-100092-2.00005-9

Bucurescu, A., Blaga, A. C., Estevinho, B. N., & Rocha, F. (2018). Microencapsulation of curcumin by a spray-drying technique using gum arabic as encapsulating agent and release studies. *Food and Bioprocess Technoloy, 11*, 1795–1806. https://doi.org/10.1007/s11947-018-2140-3

Caliskan, G., & Dirim, S. N. (2016). The effect of different drying processes and the amounts of maltodextrin addition on the powder properties of sumac extract powders. *Powder Technology, 287*, 308–314. https://doi.org/10.1016/j.powtec.2015.10.019

Carvalho, J. D. S., Oriani, V. B., de Oliveira, G. M., & Hubinger, M. D. (2019). Characterization of ascorbic acid microencapsulated by the spray chilling technique using palm oil and fully hydrogenated palm oil. *LWT, 101*, 306–314. https://doi.org/10.1016/j.lwt.2018.11.043

Chen, X., Lee, D. S., Zhu, X. & Yam, K. L. (2012). Release kinetics of tocopherol and quercetin from binary antioxidant controlled-release packaging films. *Journal of Agricultural and Food Chemistry*, *60,* 3492–3497. https://doi.org/10.1021/jf2045813

Consoli, L., Grimaldi, R., Sartori, T., Menegalli, F. C., & Hubinger, M. D. (2016). Gallic acid microparticles produced by spray chilling technique: Production and characterization. *Lebensmittel-Wissenschaft und -Technologie- Food Science and Technology, 65*, 79–87. https://doi.org/10.1016/j.lwt.2015.07.052

de Abreu Figueiredo, J., de Paula Silva, C. R., Oliveira, M. F. S., Norcino, L. B., Campelo, P. H., Botrel, D. A., & Borges, S. V. (2022). Microencapsulation by spray chilling in the food industry: Opportunities, challenges, and innovations. *Trends in Food Science & Technology, 120*, 274–287. https://doi.org/10.1016/j.tifs.2021.12.026

Estevinho, B. N., Horciu, I. L., Blaga, A. C., & Rocha, F. (2021). Development of controlled delivery functional systems by microencapsulation of different extracts of plants: *Hypericum perforatum* L., *Salvia officinalis* L. and *Syzygium aromaticum*. *Food and Bioprocess Technology, 14*, 1503–1517. https://doi.org/10.1007/s11947-021-02652-9

Fadini, A. L., Alvim, I. D., Ribeiro, I. P., Ruzene, L. G., da Silva, L. B., Queiroz, M. B., de Oliveira, A. M. R., Celio, M. F., & Rodrigues, R. A. F. (2018). Innovative strategy based on combined microencapsulation technologies for food application and the influence of wall material composition. *LWT, 91*, 345–352. https://doi.org/10.1016/j.lwt.2018.01.071

Ferrentino, G., Ndayishimiye, N., Haman, N., & Scampicchio, M. (2019). Functional activity of oils from brewer's spent grain extracted by supercritical carbon dioxide. *Food and Bioprocess Technology, 12*, 789–798.

Fu, N., You, Y. J., Quek, S. Y., Wu, W. D., & Chen, X. D. (2020). Interplaying effects of wall and core materials on the property and functionality of microparticles for co-encapsulation of vitamin E with coenzyme Q_{10}. *Food and Bioprocess Technology, 13*, 705–721. https://doi.org/10.1007/s11947-020-02431-y

Ganesan, P., & Narayanasamy, D. (2017). Lipid nanoparticles: Different preparation techniques, characterization, hurdles, and strategies for the production of solid lipid nanoparticles and nanostructured lipid carriers for oral drug delivery. *Sustainable Chemistry and Pharmacy, 6*, 37–56. https://doi.org/10.1016/j.scp.2017.07.002

Gunel, Z., Varhan, E., Koç, M., Topuz, A. & Sahin-Nadeem, H. (2021). Production of pungency-suppressed capsaicin microcapsules by spray chilling. *Food Bioscience*, *40*, 100918. https://doi.org/10.1016/j.fbio.2021.100918

Haas, K., Obernberger, J., Zehetner, E., Kiesslich, A., Volkert, M., & Jaeger, H. (2019). Impact of powder particle structure on the oxidation stability and color of encapsulated crystalline and emulsified carotenoids in carrot concentrate powders. *Journal of Food Engineering, 263*, 398–408. https://doi.org/10.1016/j.jfoodeng.2019.07.025

Haq, M., & Chun, B. -S. (2018). Microencapsulation of omega-3 polyunsaturated fatty acids and astaxanthin rich salmon oil using particles from gas saturated solutions (PGSS) process. *LWT, 92*, 523–530.

Harde, H., Das, M., & Jain, S. (2011). Solid lipid nanoparticles: An oral bioavailability enhancer vehicle. *Expert Opinion on Drug Delivery*, *8* , 1407–1424.https://doi.org/10.1517/17425247.2011.604311

Hornero-Méndez, D. & Minguez-Mosquera, M. I. (2001). Rapid spectrophotometric determination of red and yellow isochromic carotenoid fractions in paprika and red pepper oleoresins. *Journal of Agricultural and Food Chemistry, 49*, 3584-3588. https://doi.org/10.1021/jf010400l

Hoseyni, S. Z., Jafari, S. M., Tabarestani, H. S., Ghorbani, M., Assadpour, E., & Sabaghi, M. (2021). Release of catechin from Azivash gum-polyvinyl alcohol electrospun nanofibers in simulated food and digestion media. *Food Hydrocolloids*, *112*, 106366. https://doi.org/10.1016/j.foodhyd.2020.106366

Janiszewska-Turak, E. (2017). Carotenoids microencapsulation by spray drying method and supercritical micronization. *Food Research International, 99*, 891–901. https://doi.org/10.1016/j.foodres.2017.02.001

Kevij, H. T., Salami, M., Mohammadian, M., & Khodadadi, M. (2020). Fabrication and investigation of physicochemical, food simulant release, and antioxidant properties of whey protein isolate-based films activated by loading with curcumin through the pH-driven method. *Food Hydrocolloids*, *108*, 106026. https://doi.org/10.1016/j.foodhyd.2020.106026

Klettenhammer, S., Ferrentino, G., Zendehbad, H. S., Morozova, K. & Scampicchio, M. (2022). Microencapsulation of linseed oil enriched with carrot pomace extracts using particles from gas saturated solutions (PGSS) process. *Journal of Food Engineering*, *312,* 110746. https://doi.org/10.1016/j.jfoodeng.2021.110746

Klettenhammer, S., Ferrentino, G., Morozova, K., & Scampicchio, M. (2020). Novel technologies based on supercritical fluids for the encapsulation of food grade bioactive compounds. *Foods, 9*(10), 1395. https://doi.org/10.3390/foods9101395

Korsmeyer, R. W., Gurny, R., Doelker, E., Buri, P., & Peppas, N. A. (1983). Mechanisms of solute release from porous hydrophilic polymers. *International Journal of Pharmaceutics, 15*, 25–35. https://doi.org/10.1016/0378-5173(83)90064-9

de Matos-Junior, F. E., Comunian, T. A., Thomazini, M., & Favaro-Trindade, C. S. (2017). Effect of feed preparation on the properties and stability of ascorbic acid microparticles produced by spray chilling. *LWT, 75*, 251–260. https://doi.org/10.1016/j.lwt.2016.09.006

Martins, N., Roriz, C. L., Morales, P., Barros, L., & Ferreira, I. C. F. R. (2016). Food colorants: Challenges, opportunities and current desires of agro-industries to ensure consumer expectations and regulatory practices. *Trends in Food Science & Technology, 52*, 1–15. https://doi.org/10.1016/j.tifs.2016.03.009

Nabil, B., Ouaabou, R., Ouhammou, M., Saadouni, L., & Mahrouz, M. (2020). Impact of particle size on functional, physicochemical properties and antioxidant activity of cladode powder (Opuntia ficus-indica). *Journal of Food Science and Technology, 57*, 943–954. https://doi.org/10.1007/s13197-019-04127-4

Ndayishimiye, J., & Chun, B. S. (2018). Formation, characterization and release behavior of citrus oil-polymer microparticles using particles from gas saturated solutions (PGSS) process. *Journal of Industrial and Engineering Chemistry, 63*, 201–207. https://doi.org/10.1016/j.jiec.2018.02.016

Ndayishimiye, J., Ferrentino, G., Nabil, H., & Scampicchio, M. (2019). Encapsulation of oils recovered from brewer's spent grain by particles from gas saturated solutions technique. *Food and Bioprocess Technology, 13*, 256–264. https://doi.org/10.1007/s11947-019-02392-x

Okuro, P. K., de Matos, F. E. Jr. & Favaro-Trindade, C. S. (2013). Technological challenges for spray chilling encapsulation of functional food ingredients. *Food Technology and Biotechnology, 51*, 171–182.

Oliveira, E. R., Fernandes, R. V. B., Botrel, D. A., Carmo, E. L., Borges, S. V., & Queiroz, F. (2018). Study of different wall matrix biopolymers on the properties of spray-dried Pequi oil and on the stability of bioactive compounds. *Food and Bioprocess Technology, 11*, 660–679. https://doi.org/10.1007/s11947-017-2027-8

Oliveira, É. R., Fernandes, R. V. B., Botrel, D. A., Carmo, E. L., Borges, S. V. ,& Queiroz, F. (2017). Study of Different Wall Matrix Biopolymers on the Properties of Spray-Dried Pequi Oil and on the Stability of Bioactive Compounds. *Food Bioprocess Technology, 11*, 660–679. https://doi.org/10.1007/s11947-017-2027-8

Oriani, V. B., Alvim, I. D., Paulino, B. N., Procopio, F. R., Pastore, G. M., & Hubinger, M. D. (2018). The influence of the storage temperature on the stability of lipid microparticles containing ginger oleoresin. *Food Research International, 109*, 472–480. https://doi.org/10.1016/j.foodres.2018.04.066

Oriani, V. B., Alvim, I. D., Consoli, L., Molina, G., Pastore, G. M., & Hubinger, M. D. (2016). Solid lipid microparticles produced by spray chilling technique to deliver ginger oleoresin: Structure and compound retention. *Food Research International, 80*, 41–49.

Paulo, F., & Santos, L. (2019). Microencapsulation of caffeic acid and its release using a w/o/w double emulsion method: Assessment of formulation parameters. *Drying Technology, 37*, 950–961. https://doi.org/10.1080/07373937.2018.1480493

Paulo, F., & Santos, L. (2020). Encapsulation of the antioxidant tyrosol and characterization of loaded microparticles: An integrative approach on the study of the polymer-carriers and loading contents. *Food and Bioprocess Technology, 13*, 764–785. https://doi.org/10.1007/s11947-020-02407-y

Peppas, N. A., & Sahlin, J. J. (1989). A simple equation for the description of solute release. III. Coupling of diffusion and relaxation. *International Journal of Pharmaceutics, 57*, 169–172. https://doi.org/10.1016/0378-5173(89)90306-2

Pourashouri, P., Shabanpour, B., Razavi, S. H., Jafari, S. M., Shabani, A., & Aubourg, S. P. (2014). Impact of wall materials on physicochemical properties of microencapsulated fish oil by spray drying. *Food and Bioprocess Technology, 7*, 2354–2365. https://doi.org/10.1007/s11947-013-1241-2

Procopio, F. R., Ferraz, M. C., Paulino, B. N., Sobral, P. J. A., & Hubinger, M. D. (2022). Spice oleoresins as value-added ingredient for food industry: Recent advances and perspectives. *Trends in Food Science & Technology, 122*, 123–139. https://doi.org/10.1016/j.tifs.2022.02.010

Procopio, F. R., Oriani, V. B., Paulino, B. N., do Prado-Silva, L., Pastore, G. M., Sant'Ana, A. S., & Hubinger, M. D. (2018). Solid lipid microparticles loaded with cinnamon oleoresin: Characterization, stability and antimicrobial activity. *Food Research International, 113*, 351–361. https://doi.org/10.1016/j.foodres.2018.07.026

Ribeiro, A. M., Estevinho, B. N., & Rocha, F. (2019). Spray drying encapsulation of elderberry extract and evaluating the release and stability of phenolic compounds in encapsulated powders. *Food and Bioprocess Technology, 12*, 1381–1394. https://doi.org/10.1007/s11947-019-02304-z

Ritger, P., & Peppas, N. A. (1987). A simple equation for description of solute release I. Fickian and non-fickian release from non-swellable devices in the form of slabs, spheres, cylinders or discs. *Journal of Controlled Release, 5*, 23–36. https://doi.org/10.1016/0168-3659(87)90034-4

Santos, P. D. F., Rubio, F. T. V., da Silva, M. P., Pinho, L. S., & Favaro-Trindade, C. S. (2021). Microencapsulation of carotenoid-rich materials: A review. *Food Research International*, *147*, 110571. https://doi.org/10.1016/j.foodres.2021.110571

Solymosi, K., Latruffe, N., Morant-Manceau, A. & Schoefs, B. (2015). Food colour additives of natural origin. In: M.J. Scotter (Ed.). Colour additives for foods and beverages-Woodhead Publishing Series in Food Science, *279*, 3–34. https://doi.org/10.1016/B978-1-78242-011-8.00001-5

Sorita, G., Santamaria-Echart, A., Gozzo, A., Gonçalves, O., Leimann, F., Bona, E., Manrique, Y., Fernandes, I. P. M., Ferreira, I. C. F. R., & Barreiro, M. F. (2021). Lipid composition optimization in spray congealing technique and testing with curcumin-loaded microparticles. *Advanced Powder Technology, 32*, 1710–1722. https://doi.org/10.1016/j.apt.2021.03.028

Sowbhagya, H. (2019). Value-added processing of by-products from spice industry. *Food Quality and Safety, 3*, 73–80. https://doi.org/10.1093/fqsafe/fyy029

Wolska, E. (2021). Fine powder of lipid microparticles – Spray drying process development and optimization. *Journal of Drug Delivery Science and Technology*, *64*, 102640. https://doi.org/10.1016/j.jddst.2021.102640

Wejrzanowski, T., Pielaszek, R., Opalińska, A., Matysiak, H., Łojkowski, W., & Kurzydłowski, K. J. (2006). Quantitative methods for nanopowders characterization. *Applied Surface Science, 253*, 204–208. https://doi.org/10.1016/j.apsusc.2006.05.089